High Q silicon carbide microdisk resonator

Xiyuan Lu,[1] Jonathan Y. Lee,[2] Philip X.-L. Feng,[3] and Qiang Lin[2,4,a)]
[1]*Department of Physics and Astronomy, University of Rochester, Rochester, New York 14627, USA*
[2]*Department of Electrical and Computer Engineering, University of Rochester, Rochester, New York 14627, USA*
[3]*Department of Electrical Engineering and Computer Science, Case Western Reserve University, Cleveland, Ohio 44106, USA*
[4]*Institute of Optics, University of Rochester, Rochester, New York 14627, USA*

(Received 31 March 2014; accepted 28 April 2014; published online 8 May 2014)

We demonstrate a silicon carbide (SiC) microdisk resonator with optical Q up to 5.12×10^4. The high optical quality, together with the diversity of whispering-gallery modes and the tunability of external coupling, renders SiC microdisk a promising platform for integrated quantum photonics applications. © *2014 AIP Publishing LLC*. [http://dx.doi.org/10.1063/1.4875707]

Future advance of quantum photonic network relies essentially on the development of light-matter quantum interface for information processing and storage.[1] To date, a variety of approaches have been developed, based upon either photon-atom interaction in atomic gases,[1] photon-ion interactions in doped crystals,[2] or photon-spin interaction in semiconductors.[3] Recently, point defects in silicon carbide (SiC) (Refs. 4–6) were shown to possess remarkable spin coherence and near-infrared zero-phonon emission,[7,8] which led to the demonstrations of single-photon source[9] and quantum microwave emitters.[10] These superior features, together with the outstanding optical, mechanical, and thermal properties of SiC,[11] as well as the advanced wafer processing and device fabrication technology,[12–14] render SiC a promising material platform for integrated quantum photonic applications.

For this purpose, one critical underlying component is a high quality photonic device that can function as a cavity quantum electrodynamic system capable of performing strong coherent interaction between light and point defect at single quantum level.[1,15] In the past few years, considerable attention has been attracted to develop SiC photonic micro-/nano-cavities.[16–23] However, due to the significant hardness and chemical inertness, it has been quite challenging to fabricate SiC devices with photonic-grade quality. Here, we demonstrate a high-Q SiC microdisk resonator with an intrinsic optical Q of 5.12×10^4, the highest value reported to date.[16–23]

SiC is a semiconducting polymorphic material existing in more than 250 crystal structures.[11] The polytype we employed, 3C-SiC, has isotropic optical properties because of its zinc-blende (cubic) crystal structure. In particular, 3C-SiC is the only polytype that can currently be grown directly on a silicon substrate by heteroepitaxy. It is thus of a great potential for future optoelectronic integration to realize multifunctional hybrid quantum photonic circuits.

The process we employed for fabricating 3C-SiC microdisks is schematically shown in Fig. 1. First, chromium (Cr) layer with a thickness of 150 nm was deposited on top of the 3C-SiC-on-Si wafer through physical-vapor-deposition sputtering. It served as the hard mask for etching SiC with high etching selectivity. Second, the electron-beam resist ZEP520A was spin-coated on the surface of Cr mask layer and was patterned by the electron-beam lithography. The patterned device structures were then transferred to the Cr mask layer by reactive-ion etching (RIE) with chlorine plasma, which were further transferred to the 3C-SiC layer by inductively coupled-plasma RIE with fluorine-based plasma (CF_4/Ar). Fourth, the Cr mask was removed by the chromium etchant CR-14, and the silicon substrate was undercut by potassium hydroxide. The device was finally annealed at 1100 °C for 2 hours. Figure 2 shows the scanning electron microscopic (SEM) image of a fabricated 3C-SiC microdisk, with a thickness of 700 nm and a radius of 6.25 μm, sitting on the silicon pedestal. It clearly shows an improved etching quality compared with our previous devices.[20]

The fabricated microdisk was tested in a fiber-device coupling setup same as what we used previously.[20] A continuous-wave tunable laser was launched into the microdisk resonator by near-field evanescent coupling through a tapered optical fiber which also delivers the transmitted wave out of the device. The cavity transmission spectrum was obtained by scanning the laser wavelength and recording the cavity transmission accordingly. The laser wavelength was calibrated by a Mach-Zehnder interferometer.

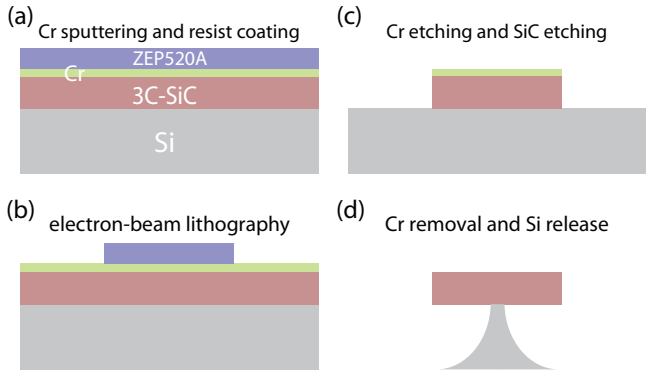

FIG. 1. Process flow for fabricating 3C-SiC microdisks.

a)Electronic mail: qiang.lin@rochester.edu.

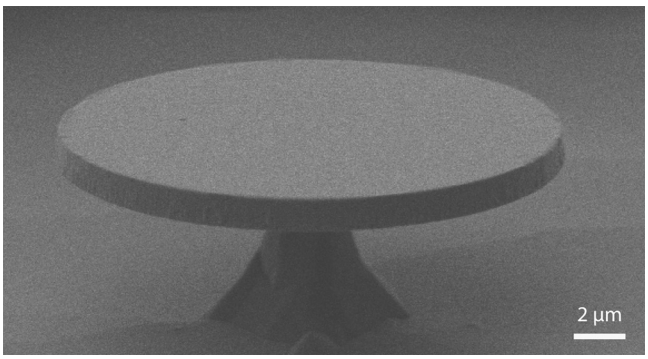

FIG. 2. SEM image of a fabricated 3C-SiC microdisk.

The testing scheme enables flexible manipulation of the external coupling of the device by adjusting the fiber-device spacing. As cavity modes of the same mode family exhibit similar external coupling to the tapered fiber and share a similar free-spectra range, mapping the cavity transmission spectra as a function of the fiber-device spacing helps identify different cavity mode families. For example, about 7 mode families are clearly observed for the quasi-transverse-electric-like (quasi-TE-like) polarization with the electric field dominantly lying in the disk plane (Fig. 3(a)), with free-spectral ranges from 22 to 26 nm. The mode species of the first 5 mode families are identified by the finite-element-method (FEM) simulations, labeled as TE1 to TE5 in Fig. 3(a), with the simulated optical mode profiles shown in Fig. 3(c). Similar for the quasi-transverse-magnetic-like (quasi-TM-like) polarization (Fig. 4(a)), the first 5 mode families

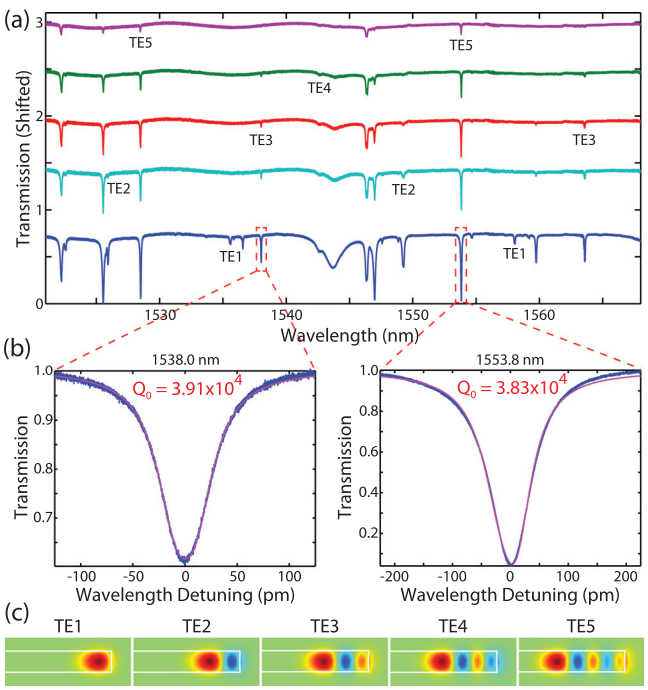

FIG. 3. (a) Cavity transmission spectrum of the quasi-TE-like polarization with the fiber-device spacing tuned from ~500 nm to 0 nm (with taper touching the device). For an easy comparison among different curves, the spectra are shifted by a value of 0.5 with respect to each other along the vertical axis. (b) Normalized transmission spectra of two cavity modes located at 1538.0 nm and 1553.8 nm, with experimental data and theoretical fitting shown in blue and red, respectively. (c) FEM-simulated optical mode profiles of the corresponding quasi-TE-like mode families.

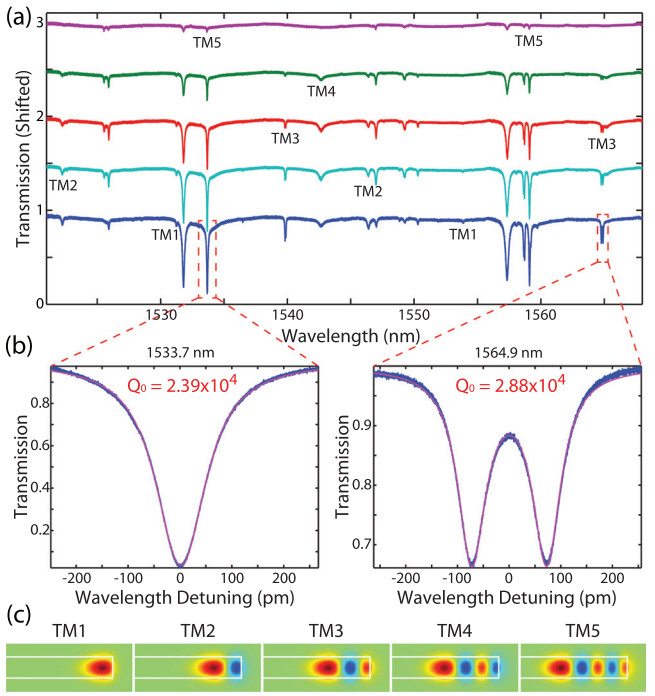

FIG. 4. (a) Cavity transmission spectrum of the quasi-TM-like polarization when the fiber-device spacing is changed. For easy comparison, the spectra are shifted by a value of 0.5 with respect to each other along the vertical axis, similar to Fig. 3(a). (b) Normalized transmission spectra of two cavity modes located at 1533.7 nm and 1564.9 nm, with experimental data and theoretical fitting shown in blue and red, respectively. (c) FEM-simulated optical mode profiles of the corresponding quasi-TM-like mode families.

are observed and labeled as TM1 to TM5 in Figs. 4(a) and 4(c), respectively. Such diversity in mode families, as a result of the high refractive index of SiC (~2.6 at a telecom wavelength), enables flexible control of cavity resonances for quantum photonic applications, as discussed in the following.

Most importantly, the optical modes in both polarizations exhibit high optical quality. Figure 3(b) shows the detailed transmission spectra of two quasi-TE-like cavity modes belonging to different mode families. They exhibit high intrinsic optical Q, with values of 3.91×10^4 and 3.83×10^4, respectively. Similar optical quality is observed for the quasi-TM-like polarization. As shown in Fig. 4(c), the two quasi-TM-like cavity modes show intrinsic optical Q of 2.39×10^4 and 2.88×10^4, respectively. The slightly lower optical Q for the quasi-TM-like polarization is likely due to their higher sensitivity to the disk surface compared with the quasi-TE-like polarization (Figs. 3(c) and 4(c)). In particular, the highest optical Q appears on the cavity modes with a certain hybridized polarization, as shown in Fig. 5. For example, the cavity resonance located at 1551.0 nm exhibits an intrinsic optical Q of 5.12×10^4. The FEM simulations show that all these cavity modes exhibit radiation-limited Q above 10^8. Therefore, the optical quality in the current device can be further improved by optimizing the fabrication process, especially the etching recipe, to reduce the sidewall roughness.

The high optical quality of the SiC microresonator paves the way towards realizing strong coupling between a point defect and a photon. A critical challenge for this purpose lies

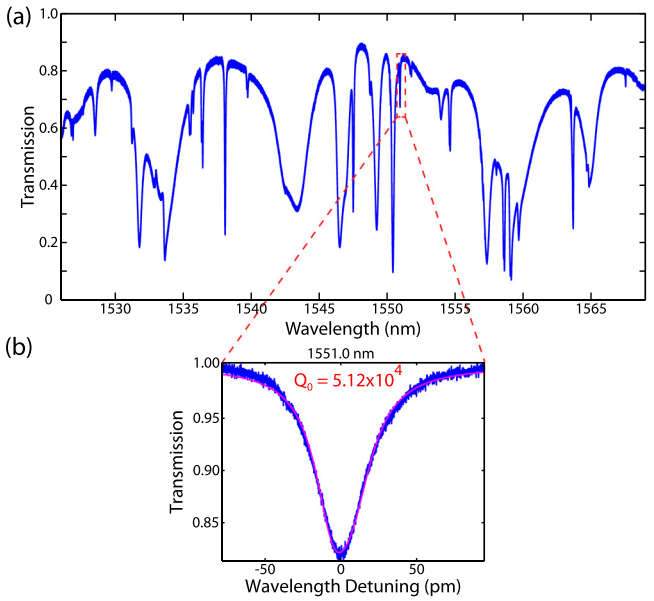

FIG. 5. (a) Cavity transmission spectrum of a hybridized polarization. The spectrum was recorded when the tapered fiber was attached to the device. (b) Normalized transmission spectrum of the cavity mode located at 1551.0 nm, with experimental data and theoretical fitting shown in blue and red, respectively.

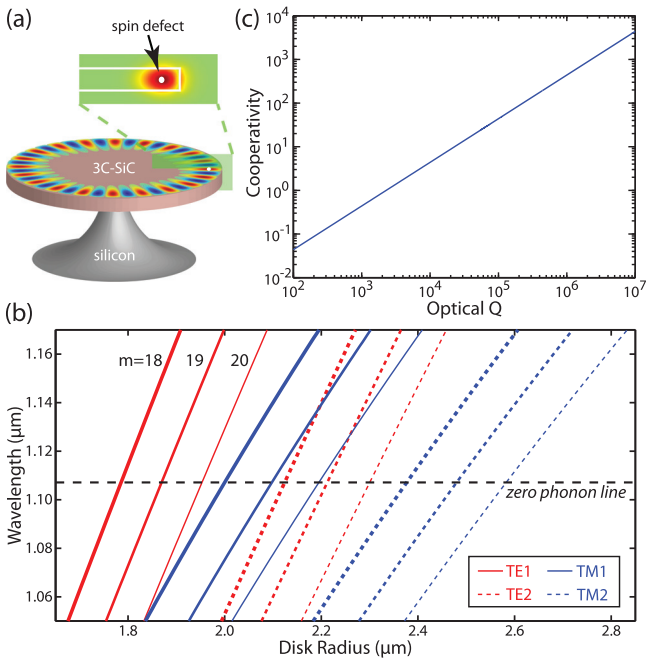

FIG. 6. (a) Schematic of a 3C-SiC microdisk resonator with a spin defect overlapping with a cavity mode. (b) FEM-simulated cavity resonances as a function of disk radius, for cavity modes with azimuthal mode number of 18, 19, 20, in both quasi-TE-like and quasi-TM-like polarizations. The dashed line indicates the wavelength corresponding to the zero-phonon emission line of the silicon-carbon divacancy center in 3C-SiC.[8] (c) Calculated cooperativity parameters for a 3C-SiC microdisk with a thickness of 300 nm and a radius of 1.87 μm, assuming $|\mathbf{E}(\mathbf{r}_d)/\mathbf{E}(\mathbf{r}_m)| = 1$.

in the difficulty in coinciding a single point defect with the maximum electric field of an optical mode.[24–26] A unique feature of the microdisk resonator is that it supports multiple mode families with different radial orders, as shown in Figs. 3(c) and 4(c). These mode families form a complete set of spatial mode distributions along the radial direction of the microdisk. With the whispering-gallery nature of the device, the optical modes cover nearly the entire volume of the microdisk. Therefore, the point defect could easily be overlapped with a certain optical mode[27] (Fig. 6(a)).

On the other hand, it is quite challenging to match the cavity resonance with the zero-phonon emission line for realizing strong coupling.[24–26] The whispering-gallery geometry supports many cavity resonances of different azimuthal mode numbers within each mode family, with frequencies separated by a free-spectral range. The cavity resonance frequencies can be flexibly engineered by finely tuning the device radius. Figure 6(b) shows the FEM-simulated cavity-resonance tuning for four mode families. It shows that the zero-phonon line at 1.12 eV,[7,8] corresponding to a wavelength of 1108 nm, can be matched by a number of cavity modes with different device radii. This feature, in combination with a certain refined cavity tuning approach,[27–29] would enable convenient frequency matching between the cavity and the defect.

Moreover, as shown previously in Figs. 3–5, versatile external couplings, from under coupling to over coupling, can be achieved for diverse cavity modes of the microdisk, simply by changing the fiber-device spacing. Such flexible control of external coupling would resolve the light extraction issue commonly existing in material platforms with high refractive indices.[24–26]

The unique cavity-mode characteristics in both spatial domain and frequency domain, with the tunability in external coupling, make SiC microdisk an excellent platform for exploring the interaction between point defect and photon. Here, we provide theoretical estimate of potential coupling strength, which is described by the cooperativity parameter given as[15,30]

$$C = \frac{3}{4\pi^2}\left(\frac{\lambda}{n_0}\right)^3 \frac{Q}{V}\frac{\gamma_{zpl}}{\gamma_{total}}\left|\frac{\mathbf{E}(\mathbf{r}_d)}{\mathbf{E}(\mathbf{r}_m)}\right|^2, \quad (1)$$

where λ, Q, V, and n_0 are cavity wavelength, optical quality, effective mode volume, and the refractive index of 3C-SiC, respectively. γ_{zpl} is the rate of zero-phonon emission at wavelength λ and γ_{total} is the total rate of spontaneous emission. $\mathbf{E}(\mathbf{r}_d)$ and $\mathbf{E}(\mathbf{r}_m)$ represent the electric fields where the defect spin ($\mathbf{r}_d$) and the maximum electric field ($\mathbf{r}_m$) are located.

For the silicon-carbon divacancy center in 3C-SiC, zero-phonon emission rate is about 10.7% of total spontaneous emission rate (including the phonon sideband) at a temperature of 20 K.[8] FEM simulations show that a 3C-SiC microdisk with a radius of 1.87 μm and a thickness of 300 nm is able to strongly confine the TE1 optical mode at 1108 nm with an effective mode volume of only 1.4 μm^3, while simultaneously maintaining a radiation-limited optical Q over 10^8. With these values, Fig. 6(c) plots the theoretical expectation of the cooperativity parameter as a function of optical Q. It shows that, for such a small microdisk, a Q value similar to our current device would provide a cooperativity of about 20 in the strong coupling regime. An optical Q of 3×10^5 would result in a cooperativity above 100. Therefore, with further improvement in the etching process, 3C-SiC microdisk is of great promise for realizing strong coherent interaction between defect spin and optical photon.

In summary, we have demonstrated a high-Q 3C-SiC microdisk resonator with diverse mode families and tunable external coupling. The device exhibits an intrinsic optical Q up to 5.12×10^4. We have shown that 3C-SiC microdisk is a promising device platform for exploring strong interaction between defect spin and optical photon, thus of great potential for diverse integrated quantum photonic applications.

The fabrication part of the work was performed at Cornell Nanoscale Science & Technology Facility (CNF), which was supported by the National Science Foundation (Grant No. ECS-0335765). P. X. L. Feng thanks support from Case School of Engineering.

[1]H. J. Kimble, Nature **453**, 1023 (2008).
[2]H. de Riedmatten, M. Afzelius, M. U. Staudt, C. Simon, and N. Gisin, Nature **456**, 773 (2008).
[3]D. D. Awschalom, L. C. Bassett, A. S. Dzurak, E. L. Hu, and J. R. Petta, Science **339**, 1174 (2013).
[4]H. Itoh, A. Kawasuso, T. Ohshima, M. Yoshikawa, I. Nashiyama, S. Tanigawa, S. Misawa, H. Okumura, and S. Yoshida, Phys. Status Solidi A **162**, 173 (1997).
[5]E. Sörman, N. T. Son, W. M. Chen, O. Kordina, C. Hallin, and E. Janzén, Phys. Rev. B **61**, 2613 (2000).
[6]N. T. Son, P. Carlsson, J. ul Hassan, E. Janzén, T. Umeda, J. Isoya, A. Gali, M. Bockstedte, N. Morishita, T. Ohshima, and H. Itoh, Phys. Rev. Lett. **96**, 055501 (2006).
[7]W. F. Koehl, B. B. Buckley, F. J. Heremans, G. Calusine, and D. D. Awschalom, Nature **479**, 84 (2011).
[8]A. L. Falk, B. B. Buckley, G. Calusine, W. F. Koehl, V. V. Dobrovitski, A. Politi, C. A. Zorman, P. X. L. Feng, and D. D. Awschalom, Nature Commun. **4**, 1819 (2013).
[9]S. Castelletto, B. C. Johnson, V. Ivdy, N. Stavrias, T. Umeda, A. Gali, and T. Ohshima, Nature Mater. **13**, 151 (2014).
[10]H. Kraus, V. A. Soltamov, D. Riedel, S. Vath, F. Fuchs, A. Sperlich, P. G. Baranov, V. Dyakonov, and G. V. Astakhov, Nat. Phys. **10**, 157 (2014).
[11]G. L. Haris, *Properties of Silicon Carbide* (INSPEC, 1995).
[12]V. Cimalla, J. Pezoldt, and O. Ambacher, J. Phys. D: Appl. Phys. **40**, 6386 (2007).
[13]N. F. Wright, A. B. Horsfall, and K. Vassilevski, Mater. Today **11**, 16 (2008).
[14]R. Maboudian, C. Carraro, D. G. Senesky, and C. S. Roper, J. Vac. Sci. Technol., A **31**, 050805 (2013).
[15]H. J. Kimble, Phys. Scr. **T76**, 127 (1998).
[16]B.-S. Song, S. Yamada, T. Asano, and S. Noda, Opt. Express **19**, 11084 (2011).
[17]S. Yamada, B.-S. Song, T. Asano, and S. Noda, Appl. Phys. Lett. **99**, 201102 (2011).
[18]S. Yamada, B.-S. Song, T. Asano, and S. Noda, Opt. Lett. **36**, 3981 (2011).
[19]S. Yamada, B.-S. Song, J. Upham, T. Asano, Y. Tanaka, and S. Noda, Opt. Express **20**, 14789 (2012).
[20]X. Lu, J. Y. Lee, P. X. L. Feng, and Q. Lin, Opt. Lett. **38**, 1304 (2013).
[21]J. Cardenas, M. Zhang, C. T. Phare, S. Y. Shah, C. B. Poitras, B. Guha, and M. Lipson, Opt. Express **21**, 16882 (2013).
[22]M. Radulaski, T. M. Babinec, S. Buckley, A. Rundquist, J. Provine, K. Alassaad, G. Ferro, and J. Vuckovi, Opt. Express **21**, 32623 (2013).
[23]A. P. Magyar, D. Bracher, J. C. Lee, I. Aharonovich, and E. L. Hu, Appl. Phys. Lett. **104**, 051109 (2014).
[24]I. Aharonovich, A. D. Greentree, and S. Prawer, Nat. Photonics **5**, 397 (2011).
[25]L. Childress and R. Hanson, MRS Bull. **38**, 134 (2013).
[26]M. Loncar and A. Faraon, MRS Bull. **38**, 144 (2013).
[27]K. Srinivasan and O. Painter, Nature **450**, 862 (2007).
[28]K. Hennessy, A. Badolato, A. Tamboli, P. M. Petroff, E. Hu, M. Atature, J. Dreiser, and A. Imamoglu, Appl. Phys. Lett. **87**, 021108 (2005).
[29]A. Faraon and J. Vuckovic, Appl. Phys. Lett. **95**, 043102 (2009).
[30]C. Santori, P. E. Barclay, K. M. C. Fu, R. G. Beausoleil, S. Spillane, and M. Fisch, Nanotechnology **21**, 274008 (2010).